Structural Determinants of Spectral Tuning in Retinal Proteins—Bacteriorhodopsin vs Sensory Rhodopsin II[#]

Shigehiko Hayashi,[†,‡] Emad Tajkhorshid,[‡] Eva Pebay-Peyroula,[§] Antoine Royant,[§,||] Ehud M. Landau,[⊥] Javier Navarro,[⊥] and Klaus Schulten*[,‡]

Beckman Institute, University of Illinois at Urbana-Champaign, 405 North Mathews, Urbana, Illinois 61801, Institute de Biologie Structurale, CEA-CNRS-Université Joseph Fourier, 41 rue Jules Horowitz, F-38027 Grenoble Cedex 1, France, European Synchrotron Radiation Facility, 6 rue Jules Horowitz, BP 220, F-38043 Grenoble Cedex, France, and Membrane Protein Laboratory, Department of Physiology and Biophysics, and Sealy Centers for Structural Biology and Molecular Science, The University of Texas Medical Branch, 301 University Boulevard, Galveston, Texas 77555-0641

Received: April 11, 2001; In Final Form: June 27, 2001

The mechanism of spectral tuning in the rhodopsin family of proteins, that act as light-driven proton (ion) pumps and light detectors, has been investigated by a combined ab initio quantum mechanical/molecular mechanical technique. Calculations are performed on two members of the family, bacteriorhodopsin (bR) and sensory rhodopsin II (sRII), for which crystal structures of high resolution are available, to explore the physical mechanisms of spectral tuning. Despite a high degree of similarity in the three-dimensional structure, electrostatic environments in bR and sRII differ sufficiently to shift absorption maxima of their common chromophore, a retinal bound to a lysine via a protonated Schiff base, from 568 nm in bR to 497 nm in sRII. This spectral shift, involving the electronical ground state (S_0) and first excited state (S_1) of retinal, is predicted correctly within 10 nm. The spectral shift can be attributed predominantly to a change in polarization of the S_1 state, and is induced predominantly by a shift of the G helix that renders the distance between the Schiff base nitrogen of retinal and the Asp201 counterion shorter in sRII than in bR. A second, weakly allowed excited state, S_2, is predicted to lie energetically close to S_1, at 474 nm. Its energetic proximity to the S_1 state suggests strong vibronic coupling and explains a shoulder observed at 457 nm in the sRII spectrum.

1. Introduction

The rhodopsin family of receptors is among the best characterized membrane proteins. These proteins reside in the cell membrane, and function as energy converters as well as sensors of light. For example, in bacteriorhodopsin (bR) of *Halobacterium salinarum*, the energy of absorbed light is used through an initial all-trans → 13-cis photoisomerization reaction of the retinal chromophore to establish an electrochemical gradient across the membrane. In rhodopsin, a common visual receptor, an initial 11-cis → all-trans retinal photoisomerization induces a signaling state of the protein that is amplified biochemically through interaction with the G protein transducin.[1]

These receptors consist of an apoprotein (opsin) and a retinal chromophore covalently bound to the apoprotein by a protonated Schiff base linkage to a lysine residue on helix G. While the protonated Schiff base form of retinal absorbs at about 440 nm in organic solvents, its maximal absorption (λ_{max}) is drastically changed after binding to the apoprotein, an effect known as "opsin shift".[2] Observed absorption maxima range from 360 to 635 nm.[3] A fundamental challenge in vision research has been the elucidation of the physical mechanisms by which the protein matrix adjusts λ_{max} of the chromophore, using the molecule retinal to absorb light at different wavelengths. Visual receptors are a good example for spectral tuning; the cone cells of the human retina contain pigments absorbing in the blue (425 nm), green (530 nm), and red (560 nm) regions of the spectrum providing the physical basis for the sense of color.[4−6] In all these pigments, the 11-cis form of retinal plays the role of the chromophore; differences in the protein matrixes bring about the spectral shifts.

Until recently, explanations for this spectral tuning were speculative. The availability of the structures of two homologous retinal proteins, bacteriorhodopsin (bR),[7−11] a light-driven proton pump, and sensory rhodopsin II (sRII),[12] a photoreceptor, with spectral maxima of 568 and 497 nm, respectively, makes it possible to compute the spectral shift and, thereby, identify the underlying physical mechanism of spectral tuning. Figure 1 compares the polypeptide sequence of sRII with that of bR. One can recognize the overall homology of the proteins as well as the conservation of most residues constituting the binding pocket of retinal.

The diversity of absorption maxima of rhodopsins has been investigated extensively[13−17] and several explanations have been proposed (for recent references, see ref 18). Most suggestions invoke electrostatic interactions between the protein matrix together with bound water molecules and the chromophore. These interactions influence ground and excited states differently, thereby, altering the excitation energy. Accordingly, the λ_{max} of retinal is adjusted by replacing amino acids, in particular

* Corresponding author. E-mail: kschulte@ks.uiuc.edu.
[†] Research fellow of the Japan Society for the Promotion of Science.
[‡] University of Illinois at Urbana-Champaign.
[§] CEA-CNRS-Université Joseph Fourier.
[||] European Synchrotron Radiation Facility.
[⊥] University of Texas Medical Branch.
[#] The authors dedicate this paper to Peter Kollman in admiration and gratitude for his ground-breaking contributions to classical and quantum mechanical studies of proteins.

10.1021/jp011362b CCC: $20.00
Published on Web 08/30/2001

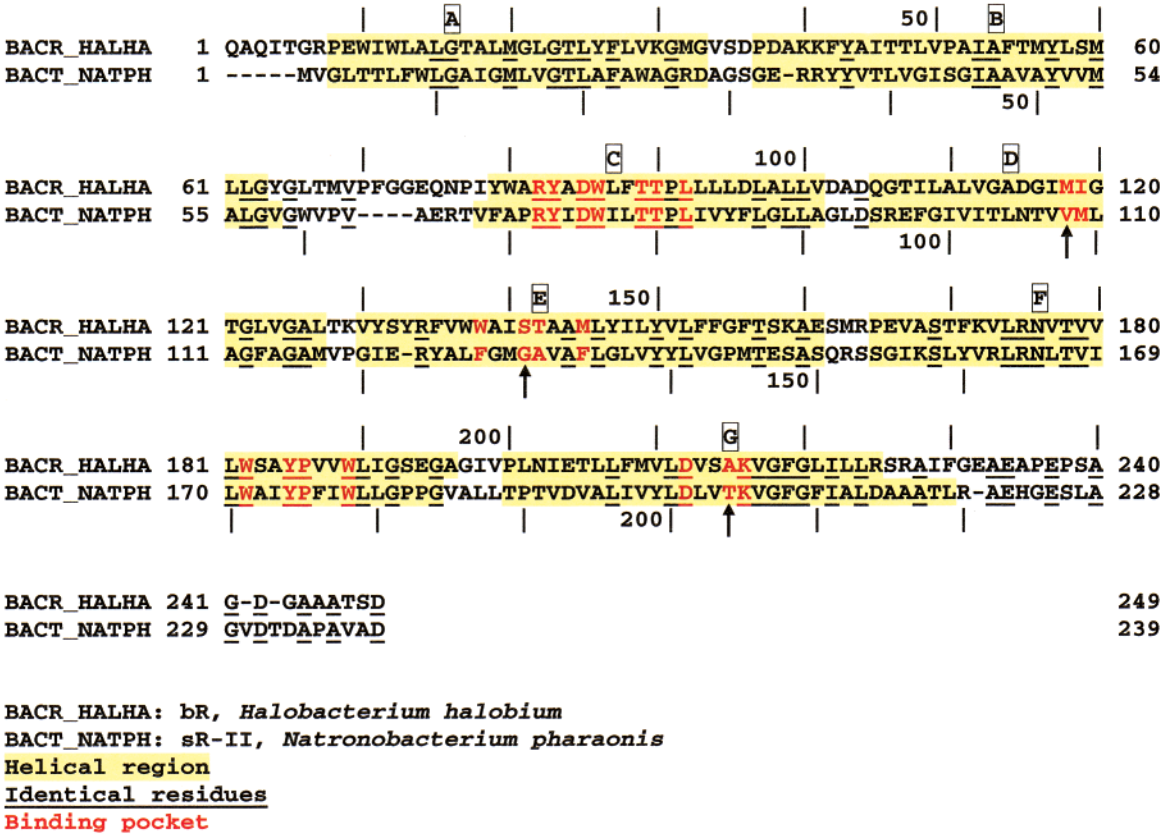

Figure 1. Comparison of bacteriorhodopsin (*Halobacterium salinarum*) and sensory rhodopsin II (*Natronobacterium pharaonis*) sequences. The alignment is based on structures of the proteins. Identical residues are underlined. Helical regions (the seven trans-membrane helices of the protein, A to G, shown in squares) are marked in yellow, and amino acids comprising the binding pocket of retinal are shown in red. Three amino acids, considered to constitute the essential differences in the chromophore binding pocket, are indicated by arrows.

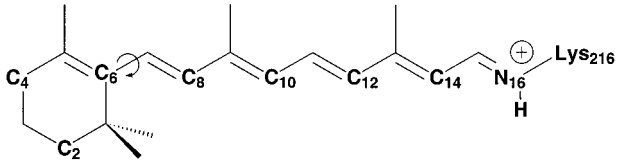

Figure 2. Schematic presentation of all-trans retinal bound via a protonated Schiff base to Lys216 in bR, and its conventional atom numbering. The possible rotation of the β-ionone ring around the C_6-C_7 single bond is highlighted; results in this paper suggest that the β-ionone ring is actually coplanar with the retinal C_7-N_{16} backbone, both in bR and sRII.

those in retinal's binding pocket. The genetics of color blindness[19,20] and proteorhodopsin phototrophy[17] are particularly fruitful sources of information in this regard.

Figure 2 shows the schematic chemical structure of retinal in bR, which is covalently connected to a lysine moiety via a protonated Schiff base linkage. Electronic excitation following light absorption significantly changes the molecule's charge distribution; the positive charge of the molecule, which in the ground state is mainly located near the Schiff base region, shifts toward the β-ionone ring (Figure 2) of retinal upon excitation.[21] Therefore, a shorter distance between the protonated Schiff base group ($C{=}N^+$) and negatively charged groups of the counterion, e.g., Asp85 and Asp212 in bR, leads to a blue-shifted spectrum.[13,22,23] This effect of the counterion has been verified by measurement of the spectra in modified species of bR, where the negative charge of the counterion had been neutralized by decreasing the pH (protonation of the anionic residue)[24] or by replacement of the residues in mutation experiments.[25] These modified pigments exhibit substantial increases of their λ_{max} values, an effect which can be almost completely reversed by introducing a negative charge into the retinal binding pocket, e.g., through the addition of high concentration of chloride.[25] Although the main electrostatic field in the retinal binding pocket is expected to originate from the negatively charged groups of the counterion, contributions from polar residues proved to be important, too. For example, in a double mutant of sRII, where a polar residue close to the Schiff base region had been replaced by a neutral one (T204A) and an apolar residue close to the β-ionone ring had been replaced by a polar one (G130S), a red shift of about 15 nm has been reported.[26]

Sterical interaction between retinal and protein can also affect spectral characteristics.[14] After binding to the protein, the chromophore may experience forces that distort its conformation, for example by twists around its bonds.[27] Retinal's excitation energy depends sensitively on the length of its conjugated system of π electrons; twists about single bonds along its conjugated backbone effectively shorten the conjugated π electron system and, thereby, shift the spectrum to the blue. Depending on the nature and extent of sterical interactions in the binding pocket, retinal may adopt different levels of nonplanarity in different proteins, reflected by different λ_{max} values. Recent X-ray structures of bR,[7-11] halorhodopsin (hR),[28] and rhodopsin (Rh),[29] resolved structural differences of retinal's β-ionone moiety (Figure 2); in the case of bR and hR the β-ionone ring is coplanar with the polyene backbone of the chromophore; in the case of Rh a twist around the C_6-C_7 single bond results in a nonplanar ring−chain conformation. Ring−chain coplanarity of the retinal was concluded also for sRII in a retinal analog study and altered retinal-protein interactions were proposed to be responsible for its significant blue shift.[30,31]

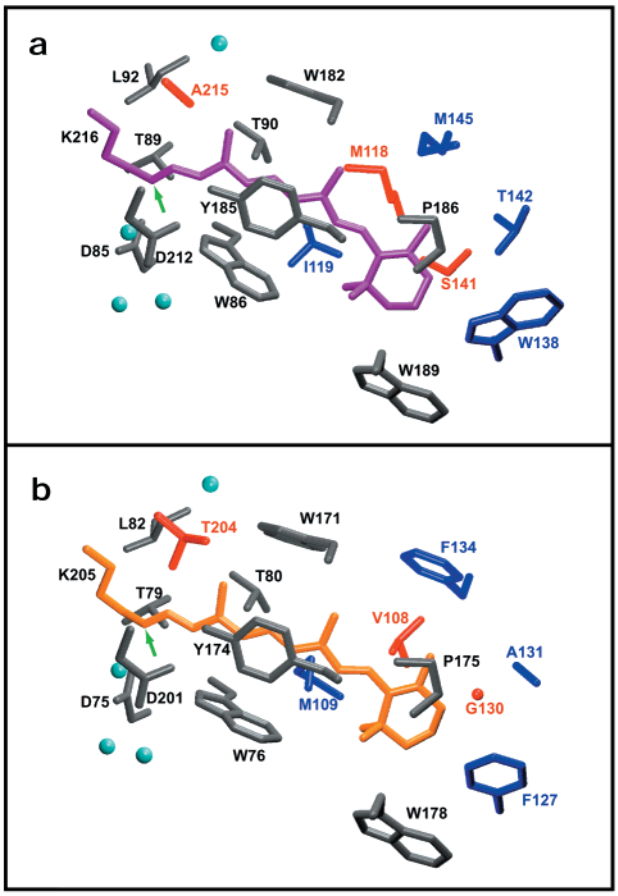

Figure 3. Comparison of the retinal binding pocket in bR (a)[10] and sRII (b).[12] Corresponding side chains in bR and sRII are shown in black when the amino acids are identical, e.g., Trp86 (bR) and Trp76 (sRII); otherwise they are shown in color, e.g., Trp138 (bR) and Phe127 (sRII). Three amino acids that are suggested to be the main contributors to the difference in maximal absorption of bR and sRII are shown in red, i.e., Ala215, Met118, Ser141 (bR), and Thr204, Val108, Gly130 (sRII). Water molecules are represented as blue spheres. Green arrows point to the nitrogen atoms of the Schiff base groups.

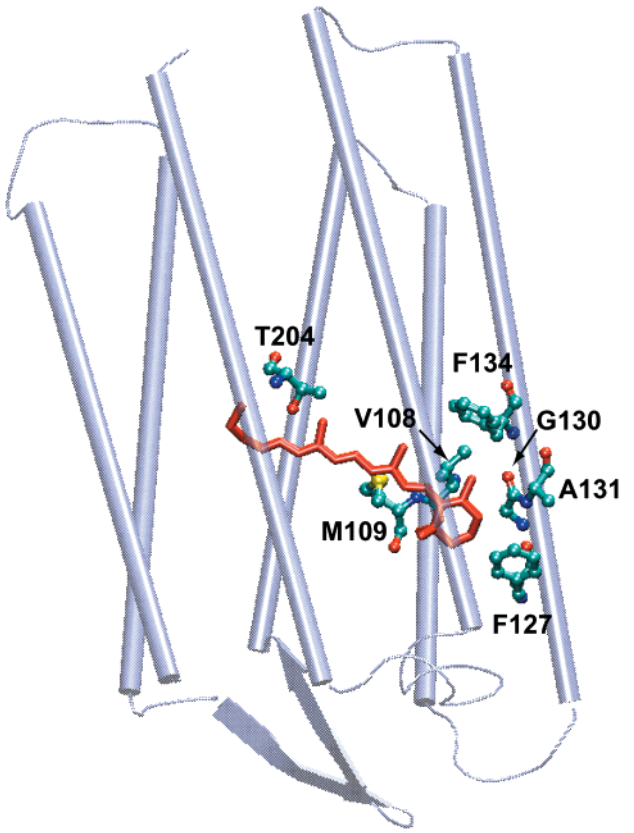

Figure 4. Structure of sRII. The seven trans-membrane helices are shown as cylinders; loops are shown in tube representation; β-strands are drawn as ribbons. The retinal chromophore is shown in red. The amino acids in the binding pocket that differ from bR are highlighted in van der Waals presentation.

The present study is an attempt to examine the spectral shift mechanisms outlined. The recent X-ray structure of sRII from *Natronobacterium pharaonis* has provided us with the necessary protein structural information.[12] The analysis is made possible because of the large degree of homology between bR and sRII that permits one to ignore computational inaccuracies which contribute the same error to bR and sRII and, hence, cancel out in the analysis of the relative spectral shift. We note here that the spectrum of sRII exhibits a characteristic shoulder structure[31,32] that needs to be explained as well, providing an opportunity to judge the quality of the computational results.

Section 2 briefly surveys key features of the recently published X-ray structure of sRII;[12] Section 3 describes the computational methods employed; the results are discussed in Section 4; and conclusions are presented in Section 5.

2. Structural Features of sRII

Figure 3 compares the retinal binding sites in bR and sRII. One can recognize readily the close structural similarities between the binding pockets in the two proteins, in particular, in regard to the packing of polarizable (aromatic) side groups around retinal. However, the proteins also differ in key side groups in the binding pocket as discernible in Figure 3. Figure 4 shows the entire structure of sRII with its seven trans-membrane helices; the side groups in sRII that differ from those in bR are highlighted. These include, in particular, the replacement of a methionine residue (Met118 in bR), a highly conserved residue among bacteriorhodopsins of different species, by a valine residue in sRII (Val108). As can be seen in Figure 3, this residue is close to retinal's β-ionone ring (cf., Figure 2). In solution, the retinal chromophore adopts a twisted 6*s*-cis ring−chain conformation. In bR, an all-trans, planar conformation has been observed,[33,34] suggesting that steric interaction between the β-ionone ring and its immediate environment stabilizes retinal's planar form. Met118 is likely to contribute to this interaction. Val108, which is a smaller residue, may free the β-ionone ring in sRII, permitting it to adopt the same twisted conformation as in solution. The unusually large blue shift of λ_{max} of the M118A mutant of bR[35] supports the suggested role of Met118. In the X-ray structure of sRII, however, the chromophore has an almost planar conformation (cf., Figure 3b), similar to that in bR. Therefore, a twisted ring−chain structure is unlikely to be responsible for the observed spectral shift of λ_{max} between bR and sRII. This is also in keeping with experimental results indicating that sRII does not bind 13-cis retinal,[36] whereas the M118A mutant of bR includes a large fraction of 13-cis retinal in both dark and light adapted states.[35]

A particularly significant difference between the X-ray structures of bR and sRII[10,12] is presented in Figure 5a, in which retinal chromophores of the two proteins are superimposed. In comparison to bR, a displacement of the G helix toward the cytoplasmic side can be seen in sRII, a finding that may explain the absence of dark adaptation (partial formation of 13-cis,15-syn retinal isomer) in sRII.[36] The displacement of this helix, to

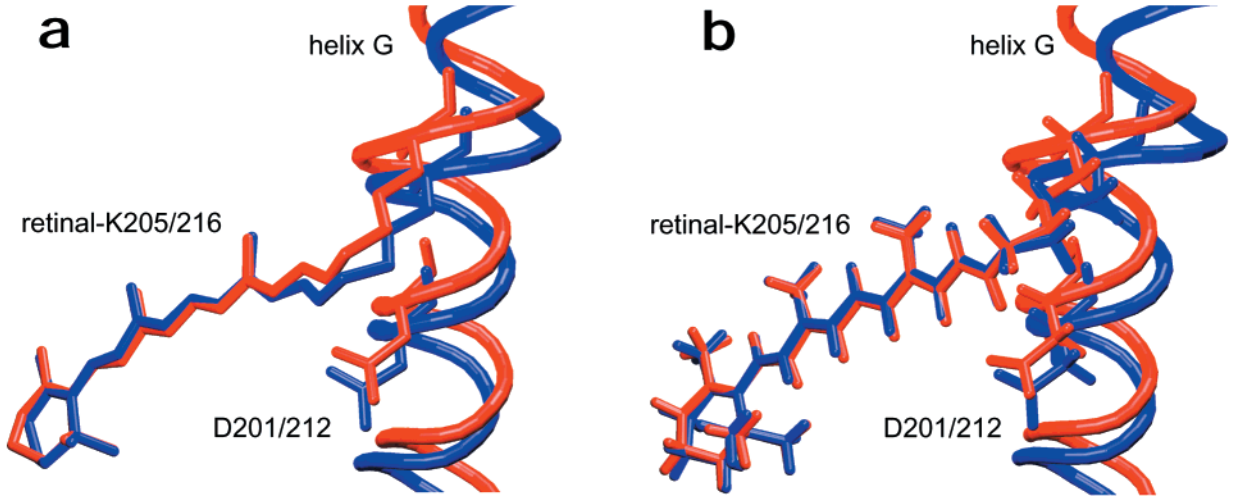

Figure 5. Comparison of crystallographic (a) and QM/MM optimized (b) structures of retinal in sRII (red) and bR (blue). Retinal-Lys205 (retinal-Lys216), Asp201 (Asp212) and helix G in sRII (bR) are displayed; helix G is shown in tube representation. In sRII, helix G is displaced toward the cytoplasmic (top) side of the membrane. In the QM/MM optimized structure, the distance (4.5 Å) between N_{16} of retinal and C_γ of Asp201 in sRII is shorter than the corresponding distance (5.2 Å) in bR. Note that in (a) hydrogens of retinal are not shown, since they are not resolved in the X-ray structures.

which the retinal is covalently bound (via a protonated Schiff base linkage to Lys205), decreases the flexibility of retinal needed to adopt the S-shape conformation of the 13-cis,15-syn isomer. Such a correlation between the chromophore isomerization and the movement of helix G is also evident from the recent X-ray structures of bR intermediates.[37−41]

Another relevant structural feature of sRII is the position of Arg72, which is pointing toward the extracellular side of the protein, in contrast to the conformation of the respective side group in bR, Arg82, which is pointing to the cytoplasmic side, i.e., toward the binding pocket of retinal. The outward orientation of Arg72 in sRII is stabilized by a salt bridge between the positively charged guanidine moiety of arginine and the negative charge located on Asp193, a residue absent in bR (Figure 1). A larger distance of the arginine side chain from the aspartate groups in the binding pocket presumably is responsible for the higher pK_a of Asp75 (5.6)[42] in sRII, as compared to that of Asp85 (2.2)[24] in bR.

3. Computational Methods

In the present study, we have applied the so-called quantum mechanical/molecular mechanical (QM/MM) methodology.[43] This approach combines conventional molecular mechanical (MM) calculations with quantum mechanical (QM) ones performed only on a specific part of the system, the retinal Schiff base and some components of its binding site. Ab initio molecular orbital methods were employed in the QM part. The QM/MM technique enabled us to calculate the optimized geometry of the whole system, as well as the excitation energy of the chromophore in the electrostatic field of the protein environment.[44−46] The QM/MM code used in our calculations is the one implemented in the program HONDO.[47] The respective calculations are described elsewhere.[45]

Models of bR and sRII were constructed using the crystal structures reported in refs 10, 11, and 12, respectively. These models contain for bR nine water molecules in the vicinity of the retinal chromophore and Arg82 (bR) and for sRII ten water molecules in the vicinity of the retinal chromophore and Arg72 (sRII), the water molecules being included in our calculation. In bR, Asp96, Asp115, and Glu204 were considered to be protonated[48,49] and the other acidic and basic residues were assumed to be charged. All titratable groups in sRII were assumed to be charged, since all of them are located in polar regions, i.e., near the surface of the protein or in the extracellular channel. The AMBER[50] force field was used for the description of the MM region, together with a 12 Å residue-based cutoff for nonbonding interactions.

Hydrogen atoms were then added and optimized with the AMBER program. Subsequently, geometry optimization for the whole system was carried out by means of QM/MM calculations. The geometry optimization of the QM region in sRII (in bR) involved the side chains of retinal-Lys205 (-Lys216), Asp75 (Asp85), Asp201 (Asp212), and water molecules W400−W402 in the binding pocket (see Figure 3). The boundaries dividing the QM and MM regions are at the $C_\beta-C_\gamma$ bond of Lys205 (Lys216) and the $C_\alpha-C_\beta$ bonds of Asp75 and Asp201 (Asp85 and Asp212). The QM regions were treated by the Hartree−Fock method during the geometry optimization. Dunning's split-valence (DZV) basis set[51] was used. In addition, diffuse functions were added on the O_δ atoms of the aspartate side chains. The number of basis functions used in the QM region was 423.

For the fully optimized geometries, the excitation energies were obtained by the complete active space self-consistent field (CASSCF) method. During the CASSCF calculation, the QM regions in both sRII and bR included only the retinal-lysine moiety. The CAS space consisted of 10 electrons in 11 valence π-orbitals. To improve the flexibility of basis functions, polarization functions were added to the C and N atoms of the polyene backbone of retinal.

4. Results and Discussion

Although the comparison of the retinal binding pocket in bR and sRII (cf., Figures 1 and 3) indicates a high degree of similarity, key amino acids differ in the two proteins. Only three of these amino acids (amino acids 108, 130, and 204 in sRII, indicated by arrows in Figure 3b) have been previously proposed to contribute significantly to retinal's 568 nm → 497 nm spectral shift. However, the replacement of all three residues in sRII by the corresponding amino acids in bR red shifts the spectrum only 497 nm → 517 nm,[26] indicating the involvement of other amino acids and of structural differences.

Figure 5, parts a and b, compare the retinal structures in bR and sRII as determined by the X-ray crystallographic studies[10,11]

TABLE 1: Absorption Maxima (nm) and the Differences of Total Energies (ΔE_{total}), Contributions of Conformational (ΔE_{ch}^{conf}), Electrostatic (ΔE_{ch-pr}^{ES}), Electronic Reorganization ($\Delta E_{ch(pr)}^{ERO}$), and Oscillator Strengths (f) in BR and SRII (Experimental values are shown in parentheses.)

			sRII-bR[e]				f	
	bR	sRII	ΔE_{total}	ΔE_{ch}^{conf}	ΔE_{ch-pr}^{ES}	$\Delta E_{ch(pr)}^{ERO}$	bR[f]	sRII[g]
S_1-S_0	(568)[a]	507[b] (497)[c]	6.1 (7.2)[a,c]	−0.3	−1.1	7.5	0.56 (0.80)[a]	0.93
S_2-S_0	(488)[a]	474[b] (457)[c,d]	1.7 (4.0)[a,c,d]	−0.8	3.1	−0.5	0.33 (0.30)[a]	0.35

[a] Ref 59. [b] Present results based on eq 1. [c] Ref 42. [d] Sideband.[42] [e] Values in kcal/mol. [f] Values determined combining the experimental absorption maxima[59] and transition dipole moments from CASSCF calculations (Table 2). [g] Values determined combining the calculated absorption maxima and transition dipole moments from CASSCF calculations (Table 3).

and by the QM/MM full geometry optimizations. In the X-ray structure of bR, retinal exhibits significant bends in the region between atoms C_{14} and N_{16} compared to that of sRII. In the QM/MM optimized structures, on the other hand, the retinal geometries in bR and sRII are very similar (Figure 5b), differing only in a slight in-plane bend of retinal's backbone in sRII.

The similarity of the positions of retinal in the two proteins, despite the movement of helix G in sRII, is related to the flexibility of the lysine residue, which connects retinal to the helix. Only slight rotations around the bonds of the chain in lysine are needed to accommodate the helix shift and to permit retinal to remain in the same position as in case of bR (Figure 5b).

The displacement of helix G, however, leads to a shift of the position of Asp201 (corresponding to Asp212 in bR), relative to the Schiff base group (Figure 5b), making the distance between N_{16} of retinal and C_γ of Asp201 in sRII (4.5 Å) shorter than the corresponding distance in bR (5.2 Å). As will be discussed below, the proximity of the counterion to the Schiff base group strongly affects the calculated absorption maximum, leading to a blue shift of the spectrum.

CASSCF calculations, using the optimized QM/MM structures and partial atomic charges, were then carried out to determine the excitation energies of retinal in bR and sRII, and to identify what features in the proteins control the spectral shift. CASSCF calculations that only include the valence π orbitals in CAS space are known to overestimate absolute excitation energies in polyenes, due to an effect related to the lack of dynamical electronic correlation between σ and π orbitals. The contribution of dynamical electronic correlation to the excitation energies was estimated by the multireference Møller−Plesset (MRMP) perturbation calculations in a previous study.[45] It was found that the excitation energies of both S_1 and S_2 states are significantly improved by taking into account the correlation effect. In the present study, however, the MRMP calculation was computationally prohibitive because we employed a larger CAS space (10 electrons in 11 orbitals) than in the previous study (12 electrons in 9 orbitals). The larger CAS space is needed to describe the highly polarized electronic wave function of retinal in sRII (see below). Because of very similar conformations of the chromophores in bR and sRII (cf., Figure 3), one expects that the corresponding error is the same for both chromophores and, hence, in a calculation of the spectral shift the errors should cancel.

In the present QM/MM calculations, electronic polarization and dispersion effects of the protein matrixes are also neglected. It is important to take into account those effects in an evaluation of absolute excitation energy because the polarization and dispersion of the environment can stabilize the chromophore in the excited states that exhibit an instantaneous change of electron density relative to that in the ground state.[13,46,52,53] The large contributions of polarization and dispersion interactions are expected to arise from aromatic residues. Houjou et al.[46] performed excitation energy calculations for bR based on the polarizable mosaic model and showed that the polarization of aromatic residues constituting the retinal binding pocket, Trp86, Trp182, and Tyr185, contributes significantly to the opsin shift. However, the contributions of the polarization and dispersion of protein matrixes in bR and sRII are expected to cancel in the calculation of the spectral shift because of the close structural similarity of the retinal binding pockets in bR and sRII (cf., Figure 3). In particular the three aromatic residues giving the dominant polarization contribution in bR (Trp86, Trp182, and Tyr185) are conserved in sRII (Trp76, Trp171, and Tyr174, respectively; see Figure 1) and their positions and conformations observed in the X-ray structures[10−12] are very similar in the two proteins.

The key results of the QM/MM CASSCF calculations, mainly in terms of differences between bR and sRII that are relevant to the explanation of the observed spectral shift, are presented in Table 1. The excitation energy in sRII is larger than that in bR by $\Delta_{sRII-bR}E_{S_1-S_0} = 6.1$ kcal/mol. Using the experimental value of λ_{max} for bR (568 nm), the absorption maximum of sRII can be obtained from the calculated $\Delta_{sRII-bR}E_{S_1-S_0}$ using

$$\lambda_{max}^{sRII}(calc) = C/(C/\lambda_{max}^{bR}(exp) + \Delta_{sRII-bR}E_{S_1-S_0}) \qquad (1)$$

where C is a known constant (2.86×10^4 nm kcal mol^{-1}). The resulting value of $\lambda_{max}^{sRII}(calc)$ is 507 nm, which is in good agreement with the experimental value of 497 nm,[42] i.e., a major part of the observed blue shift is well reproduced by the calculations.

Chromophores of the polyene family, including also retinal, are known for the existence of a second excited state, here referred to as the S_2 state, that is optically a poor absorber and lies in the energetic vicinity of the strongly absorbing S_1 excited state.[54−58] The latter gives rise to the absorption maxima at 568 and 497 nm of bR and sRII, respectively. The relative position of the weakly absorbing state is rather insensitive to environmental effects, whereas the strongly absorbing one can be significantly shifted. As a result, the relative position of the corresponding peaks in the spectra varies significantly. Once a weakly absorbing state lies close enough to a strongly absorbing one, it can usurp oscillator strength through vibronic intensity borrowing. Such a scenario seems to unfold in sRII. The difference between the S_2-S_0 excitation energies of sRII and bR is computed to be 1.7 kcal/mol (Table 1). Using the experimental value of the S_2-S_0 excitation energy of bR (488 nm),[59] and eq 1, the S_2-S_0 absorption maximum of sRII is found to be 474 nm. This places the S_2 state indeed close enough to the S_1 state to develop intensity through vibronic coupling. The S_2 state explains then naturally the shoulder in the sRII optical spectrum observed at 457 nm.[42] Indeed, the energy difference between the electronic states is well within the range of level spacing arising from the vibrational fine structures of polyenes (1450 cm^{-1}).[60]

TABLE 2: Excitation Energies, V^{ES}_{ch-pr},[a] $E^{ERO}_{ch(pr)}$ (kcal/mol),[b] Dipole Moments (in Debye), and Transition Dipole Moments (TDM, in Debye) of the Chromophore in BR

	excitation energy				dipole moment		
	gas	bR	V^{ES}_{ch-pr}	$E^{ERO}_{ch(pr)}$	gas	bR	TDM[c]
S_0			−93.2	6.2	21.1	25.9	
S_1	64.0	90.9	−77.4	17.3	1.0	10.9	8.2
S_2	95.5	106.6	−86.4	10.6	6.9	19.9	5.9, 5.0[d]

[a] Electrostatic interaction energy between the QM- and the MM-segments. [b] Electronic reorganization energy. [c] Transition dipole moment in bR. [d] Transition dipole moment between the S_1 and S_2 states.

TABLE 3: Excitation Energies, V^{ES}_{ch-pr},[a] $E^{ERO}_{ch(pr)}$ (kcal/mol),[b] Dipole Moments (in Debye), and Transition Dipole Moments (TDM, in Debye) of the Chromophore in SRII

	excitation energy				dipole moment		
	gas	sRII	V^{ES}_{ch-pr}	$E^{ERO}_{ch(pr)}$	gas	sRII	TDM[c]
S_0			−98.8	6.6	21.2	27.6	
S_1	63.7	97.0	−84.1	25.2	0.9	17.5	10.0
S_2	94.7	108.5	−88.9	10.5	6.9	20.8	6.0, 8.1[d]

[a] Electrostatic interaction energy between the QM- and the MM-segments. [b] Electronic reorganization energy. [c] Transition dipole moment in sRII. [d] Transition dipole moment between the S_1 and S_2 states.

Oscillator strengths of the absorption spectra determined from the electronic transition dipole moments calculated in the framework of the CASSCF method are also listed in Table 1. The results do not reproduce the observed increase of oscillator strength of the S_2-S_0 excitation in sRII as was actually expected. This discrepancy is due to two shortcomings. First, the energy difference between the S_1 and S_2 states of the CASSCF wave function is too large compared to the observed difference, such that the S_2 state does not mix strongly with the S_1 state. Second, our calculations do not include vibrational degrees of freedom and, hence, completely neglect vibronic couplings.

Which features of the structural differences between bR and sRII control the 568 nm → 497 nm spectral shift? To answer this question we have listed in Tables 2 and 3 the excitation energies, dipole moments, and transition dipole moments calculated for the isolated retinal Schiff base assuming for the molecule the same geometries as found in bR and sRII, respectively. The excitation energies of the isolated chromophores are almost the same, 63.7 kcal/mol for the sRII geometry and 64.0 kcal/mol for the bR geometry. The result implies that the slight geometry differences of the chromophore in sRII and bR do not contribute to the spectral shift. However, as stated above, excitation energies determined in the actual protein environments yield a spectral shift of 6.1 kcal/mol, pointing to the electrostatic field as the major controlling factor (see Table 1).

The electrostatic field generated by the protein environment has a profound effect on the excitation energy of retinal (opsin shift). In the simplest, ideal case the environment does not alter the electronic wave function of the isolated protonated Schiff base retinal, $|\Phi_0\rangle$. The Hamiltonian of the chromophore (ch) can then be separated into the electronic Hamiltonian of the isolated chromophore, $\hat{H}^0_{ch}$, and the electrostatic interaction between chromophore and protein (pr), $\hat{V}^{ES}_{ch-pr}$:

$$\hat{H} = \hat{H}^0_{ch} + \hat{V}^{ES}_{ch-pr} \tag{2}$$

In the present scenario of unaltered wave functions, the energies of electronic states would be shifted in the protein by

$$V^{ES}_{ch-pr} = \langle\Phi_0|\hat{V}^{ES}_{ch-pr}|\Phi_0\rangle \tag{3}$$

The electrostatic field of the protein, however, alters the wave function of the electronic states of retinal, the change being denoted by $|\Phi_0\rangle \rightarrow |\Phi\rangle$. The energy of the state, E_{ele}, can be decomposed then into three contributions:

$$E_{ele} = \langle\Phi_0|\hat{H}^0_{ch}|\Phi_0\rangle + [\langle\Phi|\hat{H}^0_{ch}|\Phi\rangle - \langle\Phi_0|\hat{H}^0_{ch}|\Phi_0\rangle] + \langle\Phi|\hat{V}^{ES}_{ch-pr}|\Phi\rangle \tag{4}$$

The first term accounts for the energy of isolated retinal; the second term, the so-called electronic reorganization (ERO) energy, $E^{ERO}_{ch(pr)}$,[45] accounts for the effect due to the polarization of the wave function; the third term, V^{ES}_{ch-pr}, accounts for the electrostatic interaction of the actual wave function $|\Phi\rangle$ with the protein environment.

The contributions of $E^{ERO}_{ch(pr)}$ and V^{ES}_{ch-pr} to the spectral shift in bR to sRII, presented schematically in Figure 6, are listed in Tables 2 and 3. As can be seen, the S_1-S_0 excitation energies in both sRII and bR are larger than that of isolated retinal. The dominant contributions to the blue shift of spectra in the respective protein environments stem from differences in V^{ES}_{ch-pr} between the S_1 and S_0 states, $\Delta_{S_1-S_0}V^{ES}_{ch-pr}$ (14.7 kcal/mol in sRII and 15.8 kcal/mol in bR). Figure 7 shows contributions of individual residues to $\Delta_{S_1-S_0}V^{ES}_{ch-pr}$ in sRII and bR. The results reveal that the two negatively charged aspartates (Asp75 and Asp201 in SRII, Asp85 and Asp212 in bR) make large contributions. A significant contribution stems also from the water molecule W402 directly hydrogen-bonded to the Schiff base. In case of sRII, Thr204 also contributes significantly to the blue shift (1.8 kcal/mol). This finding is consistent with the observed red-shifted spectrum of the T204A mutant,[26] where a nonpolar alanine residue replaces the polar side chain of threonine in the vicinity of the Schiff base.

Differences in the ERO energy of the S_0 and S_1 states also contribute to the increase of excitation energies (blue shift) upon placing the protonated retinal Schiff base from the gas phase into sRII or bR. As shown in Tables 2 and 3, the dipole moment of the S_1 state is more significantly changed in both bR and SRII, compared to that of the ground states. One of the most important findings of the present study is that the difference of the S_1-S_0 excitation energies in sRII and bR is mainly due to the ERO effect (Table 1). The S_1 state experiences a stronger electrostatic stabilization in sRII than in bR, leading to a smaller $\Delta_{S_1-S_0}V^{ES}_{ch-pr}$ contribution to the spectral shift (Table 1); however, this contribution is over-compensated by a large margin by the destabilizing ERO effect.

The polarization of the S_1 state in sRII is stronger than that in bR. In fact, the dipole moment of the S_1 state of sRII is larger by 6.6 D than that of bR. To examine which amino acids are responsible for the observed larger polarization of the S_1 state in sRII, we estimated the change of the electrostatic interaction of sRII upon the change of charge distribution of retinal (i.e., polarization) from bR to sRII,

$$\Delta_{q(\mathrm{sRII})-q(\mathrm{bR})}V^{ES}_{ch-pr} = \sum_{\alpha\in pr}\sum_{i\in ch}\frac{q_\alpha[q_i(\mathrm{sRII}) - q_i(\mathrm{bR})]}{r_{\alpha i}} \tag{5}$$

where q_α, q_i(sRII), and q_i(bR) are partial atomic charges of the protein part of sRII, atomic charges of retinal in sRII, and of retinal in bR, respectively. $\Delta_{q(\mathrm{sRII})-q(\mathrm{bR})}V^{ES}_{ch-pr}$ indicates how the polarization affects V^{ES}_{ch-pr}. As the electrostatic interaction between the chromophore and the protein matrix is the

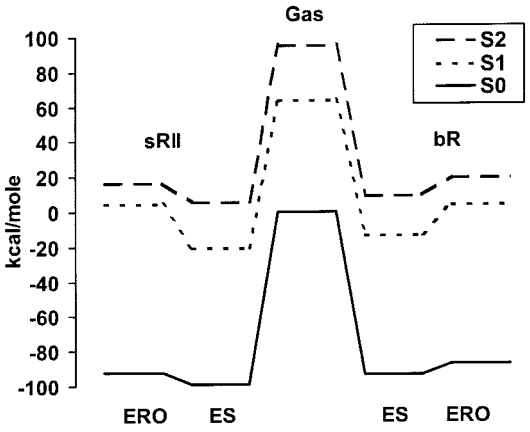

Figure 6. Graphical presentation of energy levels of the ground (S_0), first (S_1) and second (S_2) excited states of the protonated retinal Schiff base, calculated with ab initio techniques for the isolated protonated retinal Schiff base (gas phase), and for the protein bound (bR and sRII) chromophores. ES and ERO stand for electrostatic (V^{ES}_{ch-pr}) and electronic reorganization ($E^{ERO}_{ch(pr)}$) contributions to energy differences of gas-phase and protein-bound retinal, respectively (see text). Gas-phase values are used only as reference points for the contributions of ES and ERO energies, and do not correspond to any experimental values.

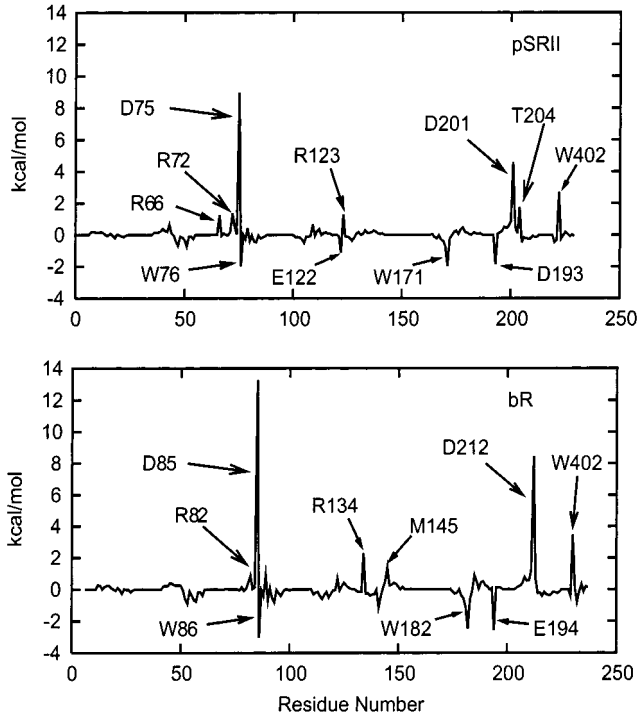

Figure 7. Electrostatic interaction energy differences between the S_0 and S_1 states, $V_{ES}(S_1) - V_{ES}(S_0)$, for the individual residues in sRII (top) and bR (bottom).

origin of the induced polarization of the chromophore, $\Delta_{q(sRII)-q(bR)}V^{ES}_{ch-pr}$ also includes the contribution of the electrostatic interaction to the polarization. Figure 8 shows $\Delta_{q(sRII)-q(bR)}V^{ES}_{ch-pr}$ of the S_1 state in sRII in terms of contributions of individual residues. One can clearly discern that the larger polarization of the chromophore in sRII results in an increase of the electrostatic stabilization by Asp201 (−6.9 kcal/mol), implying that the stronger interaction of Asp201 leads to the larger polarization. This is consistent with the above-mentioned structural difference between the chromophore binding pockets of bR and sRII, i.e., the shorter distance between

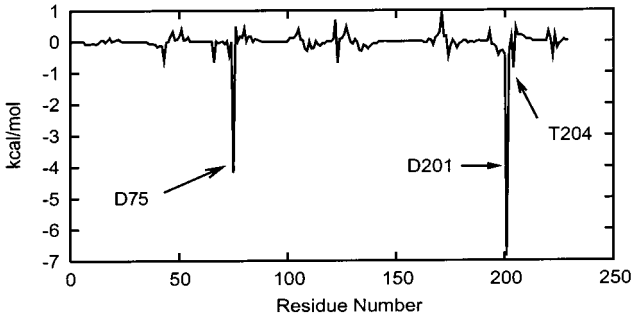

Figure 8. Electrostatic interaction and polarization contributions to the spectral shift, $\Delta_{q(sRII)-q(bR)}V^{ES}_{ch-pr}$, (see text) for individual residues of sRII. The large contribution of Asp201 indicates that the strong interaction of this residue with retinal induces in sRII the large polarization of the chromophore.

Asp201 and the nitrogen atom of the Schiff base group in sRII, in comparison to that of Asp212 in bR (see Figure 5). There also exist large contributions of stabilization by the polarization from Asp75 (−4.2 kcal/mol) and Thr204 (−0.9 kcal/mol).

The spectral shift of the S_2-S_0 excitation can be decomposed in a similar fashion. Upon excitation to the S_2 state, the positive charge in retinal moves toward the β-ionone ring. However, this charge shift is less pronounced than for the S_1-S_0 excitation and, hence, the spectrum is less affected by the electrostatic interaction. On the other hand, the energy level of the S_2 state is more sensitive to the length of the π conjugation.[58,61] Breaking the π conjugation, for example by rotation of the β-ionone ring (cf., Figure 1), results in a larger destabilization of the S_2 state compared to the S_1 state. The resulting separation of the energy levels may be responsible for the absence of a sideband in the spectrum of bovine rhodopsin despite its λ_{max} value being nearly identical to that of sRII. Indeed, a recent X-ray structure has revealed that retinal adopts a twisted ring−chain conformation in bovine rhodopsin.[29]

5. Conclusion

The mechanisms underlying spectral tuning in retinal proteins have been computationally examined for two highly homologous retinal proteins, bR and sRII, for which well-resolved structures are available, and that exhibit among themselves a strong, 568 nm → 497 nm, spectral shift. The results of our quantum mechanical calculations successfully explain the key differences between the spectra in bR and sRII. The analysis of the calculated energies shows that the observed difference is mainly due to electronic reorganization in retinal. In comparison to bR, a shift in the relative position of helix G, and, consequently, a shorter distance between the counterion and the Schiff base group of the chromophore in sRII seems to be the main reason for the observed blue shift of the spectrum. The calculated energy levels for the excited states of retinal also provide an explanation for the observed shoulder structure in the spectra of sRII. Our calculations attribute this feature to the S_2 state of retinal in sRII.

The successful explanation of the bR-to-sRII spectral shift opens the door to investigations that seek to explain on the basis of ab initio quantum chemical calculations the spectral tuning in visual pigments. For example, one may explain the optical properties of mutants of rhodopsin that display absorption spectra red- or blue-shifted relative to those of the wild type, or the spectral shift of proteorhodopsins in marine bacteria that adapt to different habitats by blue shifting with increasing aquatic depth.[17] One may finally identify the structural deter-

minants of the sense of color arising from spectral shifts among the cone pigments in the human eye.

Future studies of spectral tuning in retinal proteins should advance the methodological approach taken in the present study. A key goal should be to determine absolute excitation energies accurately by accounting for correlation effects and for polarizabilities in the protein. The latter can be achieved through adoption of atomic polarizabilities in the standard, e.g., AMBER, force field as well as through inclusion of aromatic side groups in the quantum chemical part of the QM/MM description.

Acknowledgment. S.H. is supported by the Research Fellowship of the Japan Society for the Promotion of Science for Young Scientists. The work is supported by the Roy J. Carver Charitable Trust, the National Institutes of Health (PHS 5 P41RR05969-04), the National Science Foundation (MCB-9982629), and the Human Frontier Science Program Organization. The authors also acknowledge computer time provided by the Grant NRAC:MCA93S028. J.N. and E.M.L. acknowledge support from the Welch Foundation (Grant H-1475) and the Howard Hughes Medical Institute. E.P.P. thanks the French Ministry of Education and Research (MENR). The figures in this paper were created with the molecular graphics program VMD.[62]

References and Notes

(1) Stavenga, D. G.; Grip, W. J.; Pugh, E. N. *Molecular Mechanisms in Viral Transduction*; Elsevier Science, New York, 2000.
(2) Nakanishi, K.; Crouch, R. *Isr. J. Chem.* **1995**, *35*, 253.
(3) Kleinschmidt, J.; Harosi, F. I. *Proc. Natl. Acad. Sci. U.S.A.* **1992**, *89*, 9181.
(4) Young, T. *Philos. Trans. R. Soc.* **1802**, 92, 12.
(5) König, A.; Dieterici, C. *Z. Psychol. Physiol. Sinnesorg.* **1893**, *4*, 241.
(6) Ebrey, T.; Koutalos, Y. *Prog. Ret. Eye Res.* **2000**, *20*, 49.
(7) Pebay-Peyroula, E.; Rummel, G.; Rosenbusch, J. P.; Landau, E. M. *Science* **1997**, *227*, 1676.
(8) Essen, L. O.; Siegert, R.; Lehmann, W. D.; Oesterhelt, D. *Proc. Natl. Acad. Sci. U.S.A.* **1998**, *95*, 11673.
(9) Luecke, L.; Richter, H. T.; Lanyi, J. K. *Science* **1998**, *95*, 1934.
(10) Belrhali, H.; Nollert, P.; Royant, A.; Menzel, C.; Rosenbuch, J. P.; Landau, E. M.; Pebay-Peyroula, E. *Structure* **1999**, *7*, 909.
(11) Luecke, H.; Schobert, B.; Richter, H. T.; Cartailler, J. P.; Lanyi, J. K. *J. Mol. Biol.* **1999**, *291*, 899.
(12) Royant, A.; Nollert, P.; Edman, K.; Neutze, R.; Landau, E. M.; Pebay-Peyroula, E.; Navarro, J. *Proc. Natl. Acad. Sci. U.S.A.* **2001**, in press.
(13) Irving, C. S.; Byers, G. W.; Leermaker, P. A. *Biochemistry* **1970**, *9*, 858.
(14) Baltz, P. E.; Liebman, P. A. *Exp. Eye Res.* **1973**, *17*, 573.
(15) Honig, B.; Kinur, U.; Nakanishi, K.; Balogh-Nair, V.; Gawinowicz, M. A.; Arnaboldi, M.; Motto, M. G. *J. Am. Chem. Soc.* **1979**, *101*, 7084.
(16) Schulten, K.; Dinur, U.; Honig, B. *J. Chem. Phys.* **1980**, *73*, 3927.
(17) Béjá, O.; Spudich, E. N.; Spudich, J. L.; Leclerc, M.; DeLong, E. *Nature* **2001**, *411*, 786.
(18) Lin, S. W.; Kochendoerfer, G. G.; Carroll, K. S.; Wang, D.; Mathies, R.; Sakmar, T. P. *J. Biol. Chem.* **1998**, *273*, 24583.
(19) Rattner, A.; Sun, H.; Nathans, J. *Annu. Rev. Genet.* **1999**, *33*, 89.
(20) Nathans, J. *Cell* **1994**, *78*, 357.
(21) Mathies, R.; Stryer, L. *Proc. Natl. Acad. Sci. U.S.A.* **1976**, *73*, 2169.
(22) Albeck, A.; Livnah, N.; Gottlieb, H.; Sheves, M. *J. Am. Chem. Soc.* **1992**, *114*, 2400.
(23) Livnah, N.; Sheves, M. *J. Am. Chem. Soc.* **1993**, *115*, 351.
(24) Chang, C. H.; Jonas, R.; Govindjee, R.; Ebrey, T. G. *Photochem. Photobiol.* **1988**, *47*, 261.
(25) Sasaki, J.; Brown, L. S.; Chon, Y. S.; Kandori, H.; Maeda, A.; Needleman, R.; Lanyi, K. J. *Science* **1995**, *269*, 38.
(26) Shimono, K.; Iwamoto, M.; Sumi, M.; Kamo, N. *Photochem. Photobiol.* **2000**, *72*, 141.
(27) Tajkhorshid, E.; Baudry, J.; Schulten, K.; Suhai, S. *Biophys. J.* **2000**, *78*, 683.
(28) Kolbe, M.; Besir, H.; Essen, L.-O.; Oesterhelt, D. *Science* **2000**, *288*, 1390.
(29) Palczewski, K.; Kumasaka, T.; Hori, T.; Behnke, C. A.; Motoshima, H.; Fox, B. A.; Trong, I. L.; Teller, D. C.; Okada, T.; Stenkamp, R. E.; Yamamoto, M.; Miyano, M. *Science* **2000**, *289*, 739.
(30) Hoff, W. D.; Jung, K. H.; Spudich, J. L. *Annu. Rev. Biophys. Biomol. Struct.* **1997**, *26*, 223.
(31) Takahashi, T.; Yan, B.; Mazur, P.; Derguni, F.; Nakanishi, K.; Supudich, J. L. *Biochemistry* **1990**, *29*, 8467.
(32) Imamoto, Y.; Shichida, Y.; Hirayama, J.; Tomioka, H.; Kamo, N.; Yoshizawa, T. *Photochem. Photobiol.* **1992**, *56*, 1129.
(33) Harbison, S.; Smith, S.; Pardoen, J.; Courtin, J.; Lugtenburg, J.; Herzfeld, J.; Mathies, R.; Griffin, R. *Biochemistry* **1985**, *24*, 6955.
(34) Schreckenbach, T.; Walckhoff, B.; Oesterhelt, D. *Biochemistry* **1978**, *17*, 5353.
(35) Greenhalgh, D. A.; Farrens, D. L.; Subramaniam, S.; Khorana, H. G. *J. Biol. Chem.* **1993**, *268*, 20305.
(36) Hirayama, J.; Kamo, N.; Imamoto, Y.; Shichida, Y.; Yoshizawa, T. *FEBS Lett.* **1995**, *364*, 168.
(37) Luecke, H.; Schobert, B.; Richter, H. T.; Cartailler, J. P.; Lanyi, J. K. *Science* **1999**, *286*, 255.
(38) Edman, K.; Nollert, P.; Royant, A.; Belrhali, H.; Pebay-Peyroula, E.; Hajdu, J.; Neutze, R.; Landau, E. H. *Nature* **1999**, *401*, 822.
(39) Royant, A.; Edman, K.; Ursby, T.; Pebay-Peyroula, E.; Landau. E. H.; Neutze, R. *Nature* **2000**, *406*, 645.
(40) Sass, H. J.; Buldt, G.; Gessenich, R.; Hehn, D.; Neff, D.; Schlesinger, R.; Berendzen, J.; Ormos, P. *Nature* **2000**, *406*, 649.
(41) Luecke, H.; Schobert, B.; Cartailler, J. P.; Richter, H. T.; Rosengarth, A.; Needleman, R.; Lanyi, J. K. *J. Mol. Biol.* **2000**, *300*, 1237.
(42) Chizhov, I.; Schmies, G.; Seidel, R.; Sydor, J. R.; Lüttenberg, B.; Engelhard, M. *Biophys. J.* **1998**, *75*, 999.
(43) (a) Warshel, A.; Levitt, M. *J. Mol. Biol.* **1976**, *103*, 227. (b) Warshel, A.; Chu, Z. T.; Hwang, J.-K. *Chem. Phys.* **1991**, *158*, 303. (c) Field, M. J.; Bash, P. A.; Karplus, M. *J. Comput. Chem.* **1990**, *6*, 700. (d) Gao, J. *Acc. Chem. Res.* **1996**, *29*, 298. (e) Monard, G.; Merz, K. M., Jr. *Acc. Chem. Res.* **1999**, *32*, 904, and references therein. (f) Maseras, F.; Morokuma K. *J. Comput. Chem.* **1995**, *16*, 1170. (g) Merill, G. M.; Gordon, M. S. *J. Phys. Chem. A* **1998**, *102*, 2650.
(44) Kusnetzow, A.; Singh, D. L.; Martin, C. H.; Barani, I. J.; Birge, R. R. *Biophys. J.* **1999**, *76*, 2370.
(45) Hayashi, S.; Ohmine, I. *J. Phys. Chem. B* **2000**, *104*, 10678.
(46) Houjou, H.; Inoue, Y.; Sakurai, M. *J. Phys. Chem. B* **2001**, *105*, 867.
(47) Dupuis, M.; Chin, S.; Marquez, A. In *Relativistic and electron correlation effects in molecules and clusters*; Malli, G. L., Ed.; NATO ASI Series; Plenum Press: New York, 1992.
(48) Sasaki, J.; Lanyi, J. K.; Needleman, R.; Yoshizawa, T.; Maeda, A. *Biochemistry* **1994**, *33*, 3178.
(49) Brown, L. S.; Sasaki, J.; Kandori, H.; Maeda, A.; Needleman, R.; Lanyi, J. K. *J. Biol. Chem.*, **1995**, *270*, 27122.
(50) Cornell, W. D.; Cieplak, P.; Bayly, C. I.; Gould, I. R.; Merz, K. M., Jr.; Ferguson, D. M.; Spellmeyer, D. C.; Fox, T.; Caldwell, J. W.; Kollman, P. A. *J. Am. Chem. Soc.* **1995**, *117*, 5179.
(51) Dunning, T. H., Jr.; Hay, P. J. In *Method of Electronic Structure Theory*; Shaefer, H. F., III., Ed.; Plenum Press: New York, 1977; Chapter 1.
(52) Lutzhov, V.; Warshel, A. *J. Am. Chem. Soc.* **1991**, *113*, 4491.
(53) Thompson, M. A.; Schenter, G. K. *J. Phys. Chem.* **1995**, *99*, 6374.
(54) Hudson, B. S.; Kohler, B. E. *Chem. Phys. Lett.* **1972**, *14*, 299.
(55) Schulten, K.; Karplus, M. *Chem. Phys. Lett.* **1972**, *14*, 305.
(56) Hudson, B. S.; Kohler, B. E.; Schulten, K. In *Excited State*; Lim, E. C., Ed.; Academic Press: New York, 1982; Vol. 6, p 1.
(57) Tavan, P.; Schulten, K. *J. Chem. Phys.* **1979**, *70*, 5407.
(58) Tavan, P.; Schulten, K. *Phys. Rev. B* **1987**, *36*, 4337.
(59) Birge, R. B.; Zhang, C. F. *J. Chem. Phys.* **1990**, *92*, 7178.
(60) Stern, E. S.; Timmons, C. J. In *Gillam and Stern's introduction to electronic absorption spectroscopy in organic chemistry*; The Chaucer Press: Edward Arnold, 1970.
(61) Nakayama, K.; Nakano, H.; Hirao, K. *Int. J. Quantum Chem.* **1998**, *66*, 157.
(62) Humphrey, W. F.; Dalke, A.; Schulten, K. *J. Mol. Graphics* **1996**, *14*, 33.